Optimization of a Loading System for Tissue Engineering

J. Søholm, C. Gundersen, Ø. Aune, J. Pliska, L. Christensen, M. M. Christensen

Department of Materials and Production, Aalborg University
Fibigerstraede 16, DK-9220 Aalborg East, Denmark
Email: [jplisk17, jsahol14, cgunde12, lchris13, oaune17, madchr14]@student.aau.dk
Web page: http://www.mechman.m-tech.aau.dk/

Abstract

Tissue can be grown on elastic membranes loaded by pressure. The control over the deformation of the membrane is necessary to regulate tissue growth. Different but well-defined strain states on the same membrane are desirable to enable the study of cells subjected to different conditions. This paper investigates the strain states of a silicone elastomer membrane draped over a loading post by a pneumatic hydrostatic pressure. The objective is to optimize the geometry of the loading post to achieve an equibiaxial and unidirectional strain state on a single membrane. A Finite Element Analysis of the membrane and the loading post was conducted and experimental testing of the membrane was performed. Subsequently, the optimization of the prestress of the membrane, in order to validate the FE model, and to enable the optimization of the loading post. The optimization scheme utilizes outputs of the FE model, where the geometry of the loading post is optimized to reach a desirable strain states on the membrane. Finally, a new optimized model is presented.

Keywords: **Flexcell, Membrane, Optimization, LS-DYNA, Tissue engineering, Strain**

1. General Introduction

Mechanical stimulation of cells during growth is proven to alter their cellular response, effectively altering the mechanical properties of the cells. This is utilized in the field of tissue engineering to maintain or grow new tissue, enabling replacement of damaged tissue; e.g. cartilage. Tissue can be grown on elastic membranes loaded by pressure, and the control over the deformation of the membrane is necessary to control the tissue growth. Different but well-defined strain states on the same membrane are desirable to enable the study of cells subjected to different conditions.

To govern the tissue growth, an initial premise is to understand the substrate where tissue is placed during development. The substrate investigated in this paper is a silicone membrane elastomer, which is part of a six-well culture plate provided by Flexcell. Utilizing the Flexcell FX5000 Tension system and a loading post, the membrane transfers mechanical energy to the tissue, inducing a desired mechanical strain upon the tissue. This paper builds upon the work of Grøn and Leto [1], but only the desired strain state of the membrane and geometry of the loading post is investigated and optimized. Therefore the procedure of growing cartilage is beyond the scope of this paper. The objective of this paper is contribute to the advancement of understanding and growing the artificial tissue by gaining an improved perception and control of the strain state pertaining to the membrane. The mechanical behavior of the silicone membrane in combination with the loading post is investigated with the objective of inducing an equibiaxial and unidirectional strain state on the membrane, as a uniform strain state is efficacious for the tissue growth suitable for further research. This paper is written coincidentally with a project report [2], which contains a further in-depth documentation of the subject investigated in this paper.

Assumptions and limitations of this project render the investigation of viscoelastic effects redundant, as [3] determined through experimental testing a limiting effect of viscoelastic properties for the membrane. Therefore viscoelastic properties of the membrane are assumed negligible. However, the lubricant used during the experiments could possibly induce viscoelasticity on the system [3]. Moreover, the investigation of thermal effects of the membrane has not been possible because of instrument failure. However, investigations performed by [3] determined that the mechanical properties of the membrane is temperature independent, within the range of 25°C to 37°C. Therefore thermal effects of the membrane were not investigated further, other than the discontinued experiments described in [2].

2. Models and Methods

Several different models and methods are utilized to investigate the silicone membrane including: Finite Element Method, experimental testing and optimization schemes. The FE model was established in the FE software LS-DYNA. Experimental methods were performed on the membrane to validate the FE model, which was subsequently used to optimize the geometry of the loading post.

2.1 Finite Element Model

All finite element models in this paper are generated with LS-PrePost v4.3 and solved using LS-Run v1.0. LS-DYNA utilizes an explicit solver by default, but it was chosen to use an implicit solver to better resemble the static configuration, which the membrane is subjected to during the validation experiments.
Since the FE model is utilized in an optimization scheme in MATLAB, it is important to produce a computationally efficient model by applying the symmetry conditions. The silicone elastomer membrane has a circular shape, and is therefore assumed axisymmetric, when deformed by a uniform pressure load. Employing this assumption, a quarter model of the membrane with 1960 elements is constructed, as displayed in figure 1.

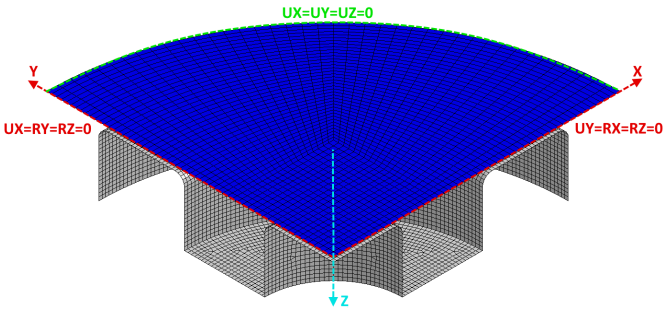

Fig. 1 Membrane FE model displaying the constraints of the model; Rotational constraint (R), Displacement constraint (U).

The contact analysis introduces nonlinearities in the FE model, so caution should be taken when utilizing symmetry in a nonlinear FE model. Moreover, investigation into the effects of symmetry is performed, however the effects of a symmetry in the model yielded equal results to the full model.
The chosen element for the membrane model is "Type 16: Full Integrated Shell Element" with a thickness of 0.508 mm, which corresponds to the dimension provided by Flexcell. The element is recommended for implicit analysis and alleviates hourglass effects [4].
The membrane model is constrained to reflect the symmetry conditions, as displayed in figure 1. The nodes at the curved edge are allowed to rotate and are constrained in all translational directions. Prestress in the membrane is simulated by reducing the original radius of the membrane model, while preserving the mesh shape and subsequently displacing the nodes of the curved edge, until the radius is equal to the original membrane radius, resulting in a uniform strain state in the membrane model.
The vacuum pressure induced by the Flexcell system is modeled as a distributed pressure load, normal to the surface of the shell elements, and the magnitude of the load matches the pressures measured in the experiments. The material of the membrane model is the LS-DYNA material model 001, which is an isotropic elastic material model. The material has a Young's modulus of 1.03 MPa and a Poisson's ratio of 0.499. Choice of material parameters is based on a tensile test preformed by [1].
Deformation of the loading post is negligible and the post is therefore modeled as a rigid shell, which is constrained in all directions. To ensure the edges of the loading post are smooth, an element radius is set to 0.20 mm. Contact between the loading post and membrane is modeled by making use of surface to surface contact, which utilizes a penalty formulation. The static and dynamic friction coefficients were set to 0.03 based on a study conducted in [2].

2.2 Experimental Work

2.2.1 Measuring Equipment

To acquire experimental data to validate the Finite Element model, a 3D laser scanning device SICK Trispector 1008 was used to measure displacement of the membrane while subjected to different constant pressures. Utilizing the laser scanning device requires the surface of the object to be matte and non-transparent. As the membrane does not pertain these properties, a talcum powder was applied on both sides of the membrane, creating a surface which the laser was incapable of penetrating and enabling a satisfactory surface image. To ensure a stable and controlled position of the laser scanner, it was mounted on a KUKA KR 6 R700 robotic arm, as depicted in figure 2.

2.2.2 Pressure Validation

Based on the incorrect pressure-displacement observations of [3] when compared to the Flexcell FX-4000 data, a validation of the pressure readings displayed by the Flexcell system was desirable. To validate the pres-

Fig. 2 Experimental setup a KUKA KR 6 R700 robotic arm with mounted TriSpector 1008 laser scanner.

sure readings, an external pressure gauge was connected in between the baseplate and the FlexLink system. The pressure gauge enabled the acquisition of real-time readings of the actual pressure flowing through the system. By doing so, the true pressure-displacement values were acquired, which was crucial for validating the Finite Element model. Only the static pressure load test were performed, utilizing the elongation [%] setting, in the FlexSoft software, as input for the experiments.

2.2.3 Pressure Settings

All experiments were performed with a vacuum level corresponding to the pressure load listed in table I. The values were obtained by averaging real-time pressure readings from the external pressure gauge for each experiment. The maximum difference in pressure readings did not exceed 0.2 kPa. The user-defined input chosen in the FlexSoft software was elongation [%], which regulates the pressure output by the FlexLink, based on the chosen regime settings in FlexSoft. All test were performed with the "25 mm loading post" regime.

Elongation [%]	1	2	3	4	5
Pressure [kPa]	6.37	11.79	16.68	21.19	25.34

Tab. I Measured pressure corresponding to the user-defined elongation setting in Flexsoft software.

The pressure was reset and the membrane unloaded before a new pressure load was applied across all experiments. In case of the experiment with the custom loading post, the maximum pressure load tested, 25.34 kPa, induced significant vibrations on the system, rendering measuring of the displacement impossible.

2.2.4 Experimental Procedure

In all the experiments, the laser scanner was centered over the well, as displayed in figure 3, and a snapshot of the membrane surface acquired for each pressure listed in table I. Measurements obtained with the TriSpector 1008 laser scanner were processed by the SOPAS Engineering Tool software provided by the manufacturer. The x-y-z coordinates of the surface were then extracted and processed using the MATLAB software.

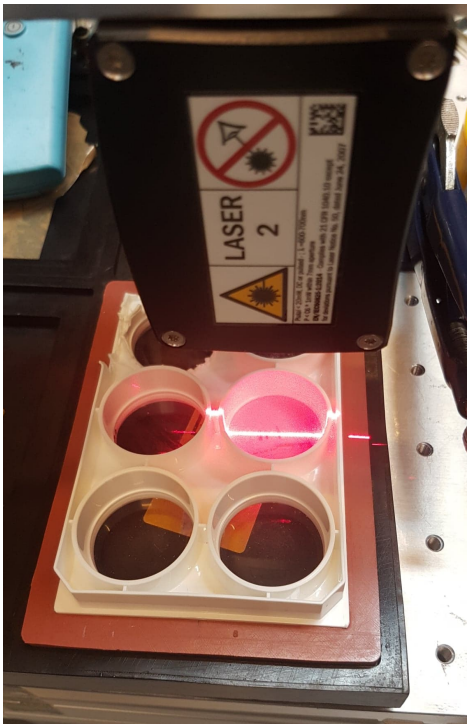

Fig. 3 The TriSpector 1008 laser scanner capturing a cross section of the membrane in the 2-well direction.

In the experiment with no loading post, two orthogonal cross-sections in the 2-well and 3-well direction, displayed in figure 3, were investigated. Each cross-section was examined in two tests:

- Test A - scanner positioned above the membrane diameter along the 2-well direction, snapshot acquired for each listed pressure in the ascending order.

- Test B - scanner position unchanged, snapshot acquired for each listed pressure in the descending order.
- Test C - scanner positioned above the membrane diameter along the 3-well direction, snapshot acquired for each listed pressure in the ascending order.
- Test D - scanner position unchanged, snapshot acquired for each listed pressure in the descending order.

In the experiment with the custom loading post, the experimental procedure remained unchanged, however only two separate tests were performed, labeled A and B, with the pressures applied in the ascending order. Silicone-based lubricant was utilized to minimize the friction between the loading post and the membrane.

2.2.5 Data Treatment

Firstly, the data are trimmed and smoothed using a robust version of local regression and utilizing weighted linear Least Squares and a second degree polynomial curve fit [5], to provide a clear view of the membrane data. Due to high computational cost of the smoothing process, the amount of data points had to be reduced by a factor of 10. Final results were obtained, by meaning over all of the valid tests. More detailed description of the data treatment can be found in chapter 4 of [2].

2.3 Optimization Methods

Two optimization schemes were performed in MATLAB. The first entails the prestress acting on the membrane, second is to optimize the geometry of the loading post. The prestress has a significant effect on the membrane properties, as illustrated in figure 4. The displacements significantly depend on the prestress, as depicted in figure 4, therefore, it could not be neglected. The improved prestressed FE model was utilized to validate the new and optimized geometry of the loading post, determined from the second optimization scheme. The prestress optimization scheme utilizes the displacements from the experimental data and variation of the prestress value, in order to coincide with the model by utilizing the Least Square method.
The tissue is placed on the membrane, when the membrane is in the prestressed configuration, therefore, the strain state of the tissue is independent of the prestress. The prestress optimization is further described in chapter 6 in [2]. This paper however, focuses mainly on the geometry optimization.

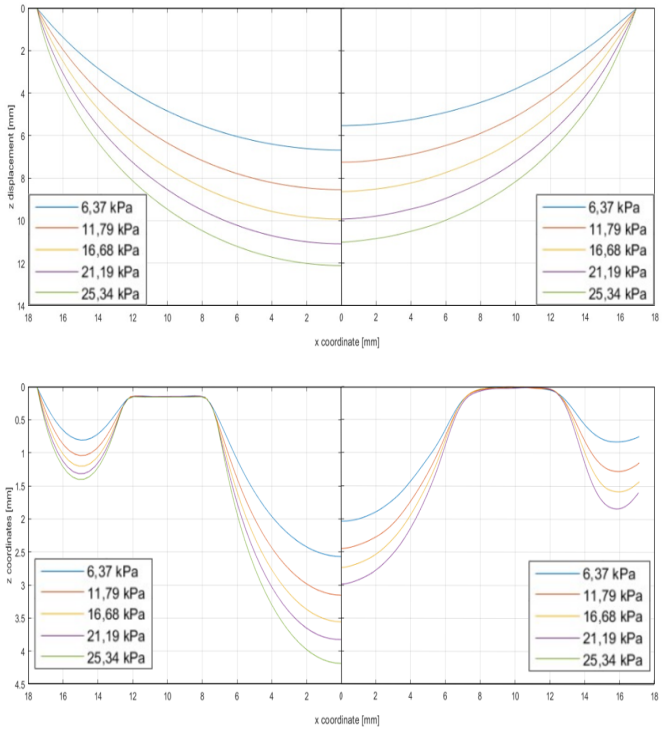

Fig. 4 Top left - non-prestress FE model with no loading post; Top right - Experimental results without loading post; Bottom left: non-prestress FE model with the non-optimized loading post; Bottom right: Experimental results with the non-optimized custom loading post

2.3.1 Geometry Optimization of Loading Post

The optimization of the loading posts is performed by utilizing the Global Weighted Sum method. The purpose of the post is to simultaneously induce an equibiaxial and uniaxial strain state at two different locations on the membrane, as depicted in figure 5.

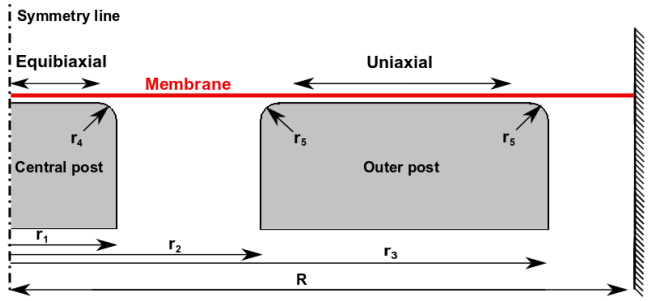

Fig. 5 Loading post and membrane with indication of radii to be optimized. Note the central post with equibiaxial strain state and outer post with uniaxial strain state.

Both strain states are described in equation (1).

$$\begin{aligned} \text{Equibiaxial:} \quad & \varepsilon_1 = \varepsilon_2, \qquad \varepsilon_3 = 0 \\ \text{Uniaxial:} \quad & \varepsilon_1 \neq 0, \qquad \varepsilon_2 = \varepsilon_3 = 0 \end{aligned} \tag{1}$$

However, as ε_2 is equal to both ε_1 and zero, see equation 1, a different approach when formulating the objective functions is required. By reformulating equation (1) into equation (2) by utilizing strain ratios of ε_1 and ε_2, rendering the cost functions dimensionless, the following equation is obtained:

$$\begin{aligned} \text{Equibiaxial:} \quad & \varepsilon_1 = \varepsilon_2 \qquad \rightarrow \frac{\varepsilon_1}{\varepsilon_2} - 1 = 0 \\ \text{Uniaxial:} \quad & \varepsilon_1 \neq 0 \quad \varepsilon_2 = 0 \rightarrow \frac{\varepsilon_1}{\varepsilon_2} = 0 \end{aligned} \tag{2}$$

Utilizing strain ratios instead of strain, enables the objective function to be established while satisfying the criteria of equation (2), as both objective functions include terms: ε_1 and ε_2. As an objective function for equibiaxial and uniaxial strain has been determined, a final objective function was established through a Summed function formulation, based on the two objective functions. The objective function of the optimization is then presented as (3), in which the objective functions of equibiaxial and uniaxial strain states were combined in the global sum function.

$$\begin{aligned} f_{obj} &= f_{equi} + f_{uni} \\ &= \left(\frac{1}{n_0} \sum^{n_0} \left(\frac{\varepsilon_1}{\varepsilon_2} - 1 \right)^2 \right)^{\frac{1}{2}} + \left(\frac{1}{n_0} \sum^{n_0} \left(\frac{\varepsilon_1}{\varepsilon_2} \right)^2 \right)^{\frac{1}{2}} \end{aligned} \tag{3}$$

The design variables of the optimization problem are the radii of the posts supporting the membrane. Inequality constraints, upper and lower bounds are established in (4).

$$\begin{aligned} & r_1 \leq r_2 - 2mm \\ & r_2 \leq r_3 - 2mm \\ & r_4 \leq 10r_1 - 0.5mm \\ & 2r_5 \leq 10r_3 - 10r_2 - 1mm \\ & \text{LB} = \quad [1, -, -, 1, 1] \qquad [mm] \\ & \text{UB} = \quad [-, -, 16.5, 25, 25] \quad [mm] \end{aligned} \tag{4}$$

3. Results and Comparison

3.1 Displacement comparison

The verification of the FE model was performed by comparison with the experimental data. An example of the comparison among the FE models, with and without prestress, and the experimental data is displayed in figure 6. Note the difference between the initial points of the experimental and FE curves. This is caused by the trimming off the transitory region of data described in chapter 4 of [2].

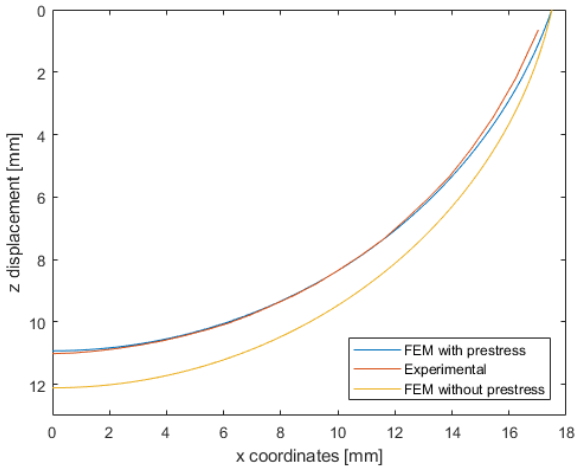

Fig. 6 The comparison of the FE models, with and without prestress, and the experimental results for the 25.34 kPa pressure load.

While the FE model with implemented prestress coincides with the experimental curve, the out-of-plane displacement of the FE displacement curve without prestress is overestimating the displacements significantly. A similar effect can be observed in the case of the custom non-optimized loading post. The model underestimates the displacements, however the difference between the model and experimental data is decreasing with increasing pressure. The displacement values for the lowest pressure load, 6.37 kPa, differ substantially. However, according to [6], only higher pressure loads are desired during normal operation of the setup. Therefore, this load case was evaluated as undesirable for optimization. Final comparison is illustrated in figure 7.

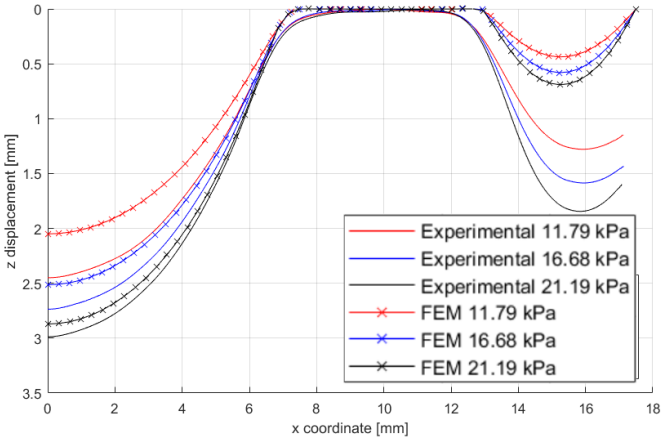

Fig. 7 Comparison of prestressed FE model and experimental data. Note the difference in size of the loading posts.

Note, that although the global displacement values of the prestressed FE model are converging to the experimental values with the increasing pressure, the local displacements are underestimated continuously in every load case. The deemed biggest factor for this deviation is that the model was set up based on the technical drawings from [1], however a direct comparison shows that the real dimensions of the post differ. This, together with the fact that these displacements are small and combined with the errors of measurements and data handling are deemed the most probable causes.

3.2 Geometry Optimization

As can be seen from figure 8, the original post aims to induce equibiaxial strain in the central hollow area. However, this solution induces a pure equibiaxial strain only at the center point, with the strain state continuously transforming into uniaxial strain on the outer post.

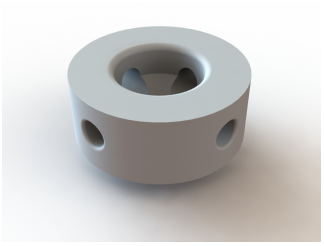

Fig. 8 Model of the original loading post introduced in [1].

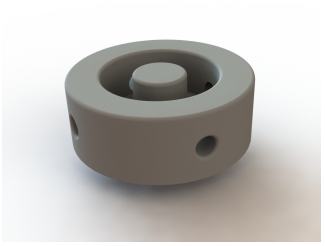

Fig. 9 Model of the geometrically optimized custom post.

Ratio	r_1	r_2	r_3	r_4	r_5
Original post $[mm]$	0	6.5	13	0	1
New post $[mm]$	4	8.67	13.67	0.50	0.56

Tab. II Comparison of the radii corresponding to figure 5.

However, with the introduction of the central post, as depicted in figure 9, the area of biaxial strain is significantly larger and well defined. Moreover, for the case of the uniaxial strain, thanks to the optimized geometry, the strain ratios acquired from the model were improved compared to the originally proposed loading post.

3.3 Strain State

The results of the optimization are presented in figure 9. The optimized post differs from the original post, depicted in figure 8, due to the implementation of the center segment. To evaluate whether the optimization was successful, the strain state of the membrane was investigated. The strain state induced by the optimized post was then compared to that of the original post, presented in figures 10 and 11, respectively. In both cases a pressure load of 21.19 kPa was applied.

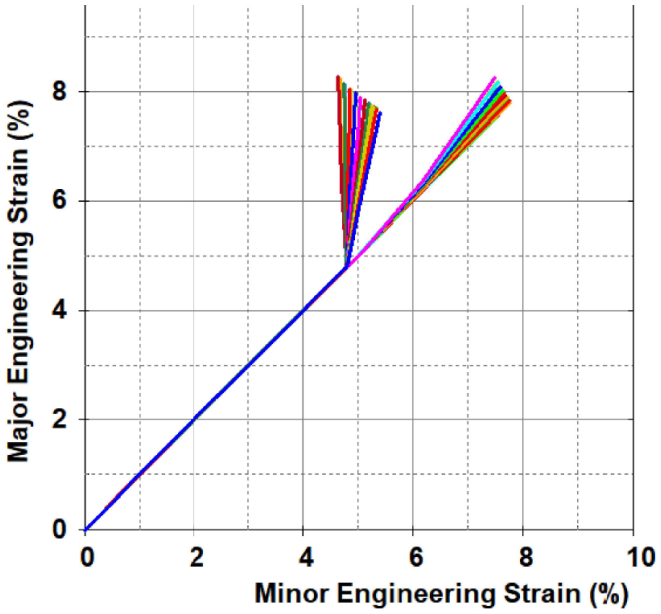

Fig. 10 Major-minor strain plots for the optimized loading post, displaying elements for both the central post and outer load post, for 21.19 kPa pressure load.

The major and minor engineering strains were utilized to evaluate which strain states are present in each element of the respective area of the membrane investigated, depicted in figure 12. The initial linear sections, depicted in figures 10 and 11, are a result of pre-tension of the membrane. The strain state is evaluated independent of the prestress due to the fact that tissue is placed on the membrane in a pre-tensioned configuration. This prestress induces an equibiaxial strain state with a major and minor strain of 4.75%.

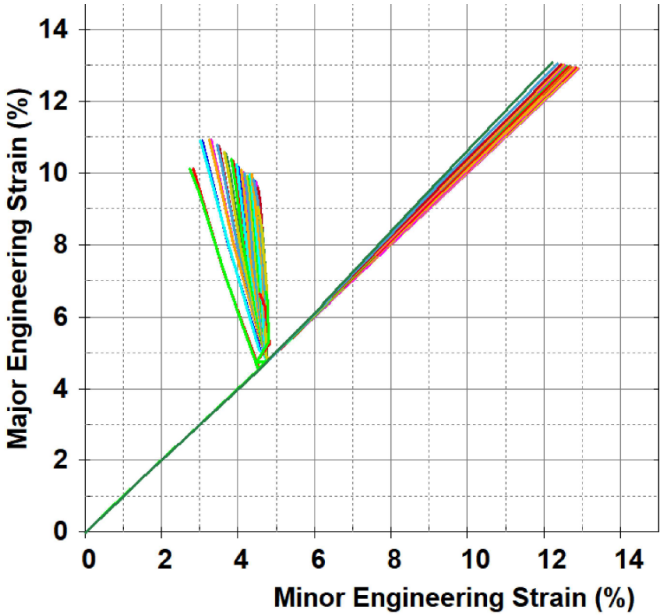

Fig. 11 Major-minor strain plots for the original post, displaying both elements for both, the central part and outer load post, for 21.19 kPa pressure load

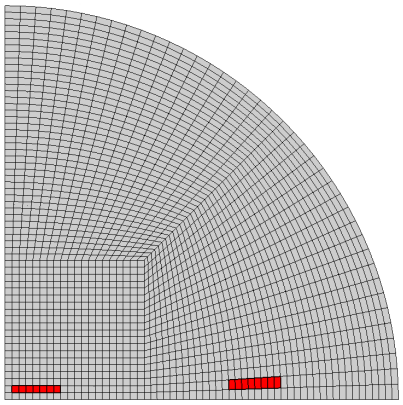

Fig. 12 FE model displaying the elements selected to investigate major and minor engineering strains.

After the initial strain segment the figures display uniaxial and biaxial behavior of the respective elements. The strain ratio is determined by comparing the change in major and minor strain with respect to the initial strain state. A big change in major strain and a small to no change in minor strain indicates an uniaxial strain state and a high strain ratio. In figure 10, a uniaxial strain state is represented as the near-vertical lines, each defining a strain state of a single element. The curves indicate that at least one element is subjected to a pure uniaxial strain state, with other elements displaying uniaxial strain with a slightly lower ratio. Correspondingly an equal change in major and minor strain indicates a biaxial strain state. The optimized post induces a more consistent uniaxial strain ratio compared to the original post, which displays greater deviation in minor strain, resulting in a lower strain ratio. The biaxial strain state is similar for both posts, with each post displaying low deviation in both minor and major strain resulting in an near equibiaxial strain state.

4. Discussion

From the initial phase of the project, the Young´s modulus is set to 1.03 MPa and Poisson´s ratio is set to 0.499. Both of these properties were presumed linear, based on the investigations conducted by [1].

The data sheets provided by Flexcell did not agree with the experimental results. Due to the complexity of the experimental setup and relatively small changes in measured parameters, the measurements are subjected to a large number of possible uncertainties and errors. Main factors influencing the accuracy of results are considered the imperfections during the data acquisition, namely the warped baseplate and therefore error in orthogonality of the laser scanner to the membrane surface, vibrations due to the Flexcell system failing to maintain a constant pressure and a difference between the pressure reading acquired from the Flexcell system and the external pressure gauge. Moreover, the data treatment process, namely trimming the transitional region of the membrane, and the smoothing and averaging process introduced a new source of error. Therefore the exact value of a total error in the measurements is difficult to determine. A solution to this problem would be to conduct a larger number of experiments and to eliminate the equipment imperfections, such as the warped baseplate.

For the FE-model, difficulties arose as it was attempted to prescribe a prestress on the system. It was concluded that the best way to prescribe the prestress was by reducing the radius of the membrane in the model, and subsequently stretching it to the original size. This process of optimization of prestress then resulted in the FE model corresponding with the results of the experimental tests. This approach was deemed satisfactory, although a different method of prescribing the prestress in the LS DYNA software might be possible.

Two optimization schemes regarding the loading post geometry were conducted. The first optimization was deemed undesirable, as the result rendered the central loading post impractical, even though it satisfied the established constraints for the system. In the second optimization, new constraints were prescribed for the

problem. This involved defining the dimensions of the central post and the thickness of the outer ring as constants, without performing an optimization study of the system. This simplified the optimization process and resulted in a more desirable design. This illustrated the importance of correctly formulating the problem which is to be optimized and even evaluating if the result, though correct, is a realistic solution or merely a numerically correct result.

5. Conclusion

The main objective of this project was to optimize the initial design of the loading post proposed by [1], used to induce well defined uniaxial and equibiaxial strain states simultaneously on a single well utilizing the Flexcell FX5000 tension system. The experimentally obtained material properties from [1] were utilized throughout the paper.

The original post used the central hollow area to induce biaxial strain. However, this solution induces a pure biaxial strain only at the center point, with the strain state changing continuously into uniaxial strain on the outer post. The optimized loading post introduced a new central section, where the area of biaxial strain is larger. Additionally, the strain ratios characterizing the uniaxial and biaxial strain states were improved by optimizing the radii of the individual posts and their edges. The goal of this paper was thereby fulfilled.

Multiple areas of interest were not investigated properly and yield an opportunity for future study, the most notable being the experimental verification of the newly optimized loading post and investigation of the strong vibrations encountered during the experimental phase of this paper. Furthermore, the magnitudes of the strains are unknown. The next step for the optimized post could, after experimental validation, be to prescribe the strain at a given pressure throughout the membrane, ensuring a specific magnitude at the posts. Moreover, further experimental testing of the unoptimized original loading post with a undeformed baseplate on multiple wells is desirable to eliminate or reduce errors during the experimental phase, together with a thorough investigation of the membrane material parameters. Finally, the classification of pressure limits, suitable for the newly proposed optimized loading post, is recommended.

Acknowledgement

The authors of this work gratefully acknowledge Grundfos for sponsoring the 6th MechMan symposium.

References

[1] A. Grøn and H. Leto, "Design of a loading post to create a unidirectional and equibiaxial strain state for the flexcell® -fx5000 tension system," 2017.

[2] Ø. Aune, L. Christensen, J. Pliska, C. Gundersen, M. Christensen, and J. Søholm, "Optimization of a loading system for tissue engineering." Project, 2018. Aalborg University.

[3] A. Colombo, P. A. Cahill, and C. Lally, "An analysis of the strain field in biaxial flexcell membranes for different waveforms and frequencies," Journal of Engineering in Medicine, vol. 222, no. 8, pp. 1235–1245, 2008.

[4] L. S. T. C. LS-DYNA, "Ls-dyna theory manual." http://www.lstc.com/pdf/ls-dyna_theory_manual_2006.pdf, 2006. Located 08-05-2018.

[5] Mathworks, "Mathworks." https://se.mathworks.com/help/curvefit/smooth.html, 2018. Located 16-05-2018.

[6] F. I. Corporation, "Flexcell fx-5000tm tension system user manual." http://www.flexcellint.com/documents/FX-5000TensionUsersManual.pdf, 2018. Located 18-03-2018.